JBMR

Identification of Quantitative Trait Loci Influencing Skeletal Architecture in Mice: Emergence of *Cdh11* as a Primary Candidate Gene Regulating Femoral Morphology

Charles R Farber,[1,2] Scott A Kelly,[3] Ethan Baruch,[1] Daniel Yu,[1] Kunjie Hua,[3] Derrick L Nehrenberg,[3] Fernando Pardo-Manuel de Villena,[3] Ryan J Buus,[3] Theodore Garland Jr.,[4] and Daniel Pomp[3,5]

[1]Center for Public Health Genomics, University of Virginia, Charlottesville, VA, USA
[2]Departments of Medicine and Biochemistry and Molecular Genetics, University of Virginia, Charlottesville, VA, USA
[3]Department of Genetics and Carolina Center for Genome Science, University of North Carolina, Chapel Hill, NC, USA
[4]Department of Biology, University of California Riverside, Riverside, CA, USA
[5]Department of Nutrition, Department of Cell and Molecular Physiology, Carolina Center for Genome Science, University of North Carolina, Chapel Hill, NC, USA

ABSTRACT

Bone strength is influenced by many properties intrinsic to bone, including its mass, geometry, and mineralization. To further advance our understanding of the genetic basis of bone-strength-related traits, we used a large ($n = 815$), moderately (G_4) advanced intercross line (AIL) of mice derived from a high-runner selection line (HR) and the C57BL/6J inbred strain. In total, 16 quantitative trait loci (QTLs) were identified that affected areal bone mineral density (aBMD) and femoral length and width. Four significant ($p < .05$) and one suggestive ($p < .10$) QTLs were identified for three aBMD measurements: total body, vertebral, and femoral. A QTL on chromosome (Chr.) 3 influenced all three aBMD measures, whereas the other four QTLs were unique to a single measure. A total of 10 significant and one suggestive QTLs were identified for femoral length (FL) and two measures of femoral width, anteroposterior (AP) and mediolateral (ML). FL QTLs were distinct from loci affecting AP and ML width, and of the 7 AP QTLs, only three affected ML. A QTL on Chr. 8 that explained 7.1% and 4.0% of the variance in AP and ML, respectively, was mapped to a 6-Mb region harboring 12 protein-coding genes. The pattern of haplotype diversity across the QTL region and expression profiles of QTL genes suggested that of the 12, *cadherin 11* (*Cdh11*) was most likely the causal gene. These findings, when combined with existing data from gene knockouts, identify *Cdh11* as a strong candidate gene within which genetic variation may affect bone morphology. © 2011 American Society for Bone and Mineral Research.

KEY WORDS: BONE MINERAL DENSITY; BONE MORPHOLOGY; BONE GEOMETRY; OSTEOPOROSIS; MOUSE GENETICS; ADVANCED INTERCROSS LINE

Introduction

Osteoporosis is a common and complex disorder characterized by bone fragility. Bone fragility is influenced by a myriad of factors, and of those intrinsic to bone, bone mineral density (BMD) and bone geometry are two of the most important.[1–3] Although these traits are influenced by both environmental and genetic factors, most (~60% to 80%) of their variance is genetically based.[4] Thus, bone fragility is primarily a genetic disorder, and studies aimed at elucidating its genetic basis are critical for the development of a comprehensive understanding of osteoporosis.

Over the last decade, the mouse has been used extensively to investigate the genetic basis of bone traits. Because of its clinical relevance, most studies have focused on BMD,[5,6] although other skeletal traits, such as bone geometry, also have been subjected to genetic analysis.[7] With regard to BMD, much of this work was summarized recently in the reanalysis of genetic data from 11 F_2 crosses that placed over 150 BMD quantitative trait loci (QTLs) on a standardized mouse genetic map.[5] To gauge the usefulness of the mouse for the discovery of BMD genes, the authors evaluated the genomic overlap between human BMD genome-wide associations (GWAs) and newly positioned mouse QTLs. Of the 28 human GWAs identified at the time, 26 overlapped with

Received in original form January 14, 2011; revised form April 11, 2011; accepted May 17, 2011. Published online June 2, 2011.
Address correspondence to: Charles R Farber, PhD, Center for Public Health Genomics, PO Box 800717, University of Virginia, Charlottesville, VA 22908, USA. E-mail: crf2s@virginia.edu

Journal of Bone and Mineral Research, Vol. 26, No. 9, September 2011, pp 2174–2183
DOI: 10.1002/jbmr.436

mouse BMD QTLs. These data suggest that there may be a significant overlap in genes harboring natural variation that perturb skeletal development and maintenance in humans and mice. In addition, human GWA studies that include upwards of 20,000 subjects have only been able to explain approximately 3% of the genetic variance for BMD,[8] and there are a number of difficulties inherent in assessing all traits that contribute to bone fragility in human populations. Therefore, it is likely that mouse genetics has much to contribute with regard to the discovery of bone fragility genes.

In this study, we used a G_4 advanced intercross line (AIL) to identify QTLs that modulate skeletal architecture. This G_4 population originated from a reciprocal cross between mice with a genetic propensity for increased voluntary exercise [high-runner (HR) line] and the C57BL/6J (B6) inbred strain.[10,14] Our analysis revealed a complex genetic architecture for both areal BMD (aBMD) and femoral morphology. Furthermore, as a step toward gene discovery, we investigated a QTL that affects femur width on chromosome (Chr.) 8 in more detail. This locus was the most statistically significant and possessed the smallest 1-LOD (LOG of odds) drop confidence interval, a region harboring only 12 genes. The combination of gene expression data and an analysis of identity by descent (IBD) suggested that of the 12 genes, *cadherin 11* (*Cdh11*) was the most likely candidate. These results increase our understanding of the genetic influences on skeletal architecture and suggest that *Cdh11* is involved in the regulation of femur morphology.

Materials and Methods

Methods relevant to the creation, phenotyping, and genotyping of the mapping population used here have been described previously.[10,14] Additionally, a complete list of the final set of single-nucleotide polymorphisms (SNPs; $n = 530$) used for the QTL analyses can be found elsewhere.[10,14] SNP locations are from Mouse Build 36 of the Mouse Diversity Genotyping Array (http://cgd.jax.org/tools/diversityarray.shtml). Only methods relevant to the current phenotypes and statistical analyses will be presented here.

Phenotypes

A moderately (G_4) AIL was generated from a reciprocal cross between mice selectively bred for high voluntary wheel running (HR) and the inbred strain C57BL/6J (B6). The HR line (one of four replicates) is the result of a long-term artificial selection experiment for high voluntary wheel running on days 5 and 6 of 6-day wheel exposure.[15] The original progenitors of the selection experiment were outbred, genetically variable house mice ($n = 224$, *Mus domesticus*, Hsd:ICR; Harlan Sprague-Dawley, Indianapolis, IN, USA). At the outset of the selection experiment, mice were mated for two generations and randomly assigned to eight closed lines (four HR lines and four control lines). These eight lines remained closed in each successive generation. HR mice in the current experiment originated from the forty-fourth generation of selection. HR mice have been the focus of numerous investigations, including those examining plasticity of hind limb bones,[16] bone morphology and mechanics,[17] within-bone stiffness,[18] and diaphyseal structure.[19] To generate the AIL employed here, the F_1 generation was intercrossed to produce an F_2 and subsequently an F_3 generation. Following the F_3 generation, a large G_4 population ($n = 815$) was generated for broad phenotype and genotype collection. In all generations, both sexes and each reciprocal cross-line population (HR♀ × B6♂ and B6♀ × HR♂) were roughly equally represented. At approximately 9 weeks of age, G_4 mice were weighed (± 0.1 g) and euthanized, and the carcasses were stored at -30°C.

Areal bone mineral density (aBMD) measures were determined using a Lunar PIXImus II densitometer (GE Healthcare, Piscataway, NJ, USA). Carcasses were thawed overnight at 4°C and placed for dual-energy X-ray absorptiometric (DXA) imagining in a prostrate fashion, with the head always in the same orientation, on an imaging positioning tray. Subsequently, whole-body scans were analyzed using the manufacturer's software (Version 2.0, Lunar Corp, Madison, WI, USA). From each DXA scan, we evaluated total aBMD (excluding the skull; TBMD), vertebral aBMD (L_1–L_5; VBMD), and femoral aBMD [(right + left)/2; FBMD]. VBMD and FBMD were obtained, using the imaging software, by placing a region of interest (ROI) over the lumbar vertebrae and around each of the left and right femurs. Previous investigations using PIXImus densitometers have documented variation in aBMD associated with positioning of the animal during imaging.[20] Accordingly, we noted the *x* and *y* coordinates for each scan and region of interest to evaluate potential positioning effects in this investigation.

Following DXA measurements, right femurs were removed, partially defleshed, wrapped in cheesecloth saturated with phosphate-buffered saline (PBS), and stored at -80°C. At a later date, femurs were partially thawed, and the three morphometric traits were measured to the nearest 0.01 mm with digital calipers. The traits were femoral length (FL), proximal tip of the femoral head to the distal-most end of the medial condyle, anteroposterior femoral width (AP) at the mid-diaphysis just below the gluteal tuberosity, and mediolateral femoral width (ML), also at the mid-diaphysis. Partial correlations were performed in SAS (Version 9.1, SAS Institute, Cary, NC, USA), controlling for parent-of-origin type, sex, and body mass. Presented *p* values were adjusted for multiple comparisons using the false-discovery-rate procedure[21] in SAS.

QTL analysis

The G_4 AIL was produced through intercrossing over multiple generations; as a result, the assumption of independence of individuals is formally incorrect, and conventional mapping methods that assume so may lead to potentially false-positive signals.[22,23] Therefore, we employed the genome reshuffling for advanced intercross permutation (GRAIP) procedure[22] to generate genome-wide significance thresholds that appropriately account for the family structure in the current AIL population. The specific details of implementation of this procedure for this population can be found elsewhere.[10,24]

We evaluated the six (TBMD, VBMD, FBMD, FL, AP, and ML) skeletal architecture traits for QTLs using R/qtl[25] for the R environment (Version 2.8.1).[26] Within R/qtl, we used the multiple-imputation method.[27] For the aBMD traits, the additive

statistical model included parent-of-origin type [whether a G_4 individual was descended from a progenitor (F_0) cross of HR♀ × B6♂ or B6♀ × HR♂, coded as 1 or 0, respectively], sex, body mass (at the time of killing), and the *x* and *y* coordinates for each specific aBMD measure. For the length and width measures, the additive statistical model included parent-of-origin type, sex, body mass, and technician (coded as 0 or 1). All factors included in both additive models have known effects on the traits of interest.

Locus-specific *p* values and genome-wide GRAIP-adjusted significance thresholds were calculated using R/qtl output from the original population and the 50,000 GRAIP-permuted populations, as described previously.[10,28] Since we employed 50,000 permutations to generate genome-wide adjusted significance thresholds, a minimum possible *p* value for the GRAIP output is 0.00002 (1/50,000) with a corresponding maximum log *p* of 4.7. Significant and suggestive loci were defined as those which met or exceeded the 95th ($p \geq .05$) and 90th ($p \geq .1$) percentiles. Confidence intervals (CIs; 90% and 95%) were approximated by 1-LOD drop support intervals (in megabases) relative to the GRAIP-permuted LOD score. In cases where the maximum GRAIP LOD score (4.7) spanned nearly the entire chromosome, CIs were estimated using the naive LOD scores. The percent of phenotypic variation accounted for by each QTL, as well as additive and dominance effects, were estimated in R/qtl.

In addition to the analyses just presented, we also investigated potential QTL × sex interactions. Significant interactions were identified as $LOD_{Full} - LOD_{Additive} = LOD \geq 3$, where the LOD_{Full} model contains the interaction term.[27]

Expression survey

In an effort to prioritize genes within candidate regions identified below (see "Results"), we examined existing microarray data and evaluated relative expression levels in primary osteoblasts and osteoclasts. For this analysis, we used previously generated microarray data that profiled a large number of mouse tissues and cell types.[29] We downloaded the raw Affymetrix MOE430 microarray data for all osteoblast and osteoclast samples from the Gene Expression Omnibus (GEO) database (www.ncbi.nlm.nih.gov/geo; accession no. GSE10246). The data consisted of two replicates for each of four samples: primary osteoblasts on days 5, 14, and 21 of differentiation and primary osteoclasts. The raw data were imported and processed using the affy R package.[30] The robust multiarray algorithim (RMA) was used to normalize and generate probe-level expression data.[31] A *t* test was used to determine the significance of differences between time points among the osteoblast samples.

Exclusion mapping analysis

For a subset of the results presented below, we further refined candidate gene regions by excluding intervals in which the haplotypes of the parental strains (ie, HR and B6) are IBD using SNPs from the Mouse Diversity array.[32] We genotyped a subset of representative individuals from the F_0 parental strains ($n = 12$, HR; $n = 1$, B6) and used SNPs to determine (1) whether the interval is homozygous or heterozygous in each sample and (2) whether samples are IBD in each homozygous interval. Briefly, we determined the frequency of heterozygous calls in windows of 200 consecutive SNPs in each one of the 12 HR individuals independently. Regions with more than 2% of SNPs with heterozygous calls were considered heterozygous based on analysis of 101 fully inbred strains from the Jackson Laboratory (Bar Harbor, ME, USA). We then tested whether regions of homozygosity in all 12 HR founders contain different haplotypes. Finally, we identified intervals that are IBD among all 12 HR founders and B6 using the same 200-SNP window and threshold (>97% genotype identity) approach used to identify the segregating regions.

Results

Descriptive statistics and partial correlations among skeletal traits are presented in Table 1. The pairwise partial correlations between aBMD and femoral geometry traits were positive and statistically significant ($p < .05$). As would be expected, TBMD was highly correlated with VBMD ($r = 0.708$) and FBMD ($r = 0.699$). In addition, FBMD and VBMD also were positively correlated ($r = 0.551$). Since aBMD is a measure of bone mineral content per unit area, we would not expect that measures of femur size and FBMD to be correlated, but the correlation between FBMD and FL was significant ($r = 0.120$, $p < .05$). Additionally, AP and ML femur widths were even more highly correlated with FBMD ($r = 0.315$ and $r = 0.294$, respectively, $p < .0001$), indicating that independent of sex, body mass, and femur length and width, areal FBMD was higher in mice with larger bones. We observed a high correlation between AP and ML ($r = 0.547$), with lower correlations between the width traits and FL ($r = 0.343$ and $r = 0.253$, respectively), suggesting that

Table 1. Descriptive Statistics and Partial Correlations for Skeletal Architecture Traits in the G_4 Population

Trait	*n*	Mean	SD	Range	Femoral BMD	Vertebral BMD	Total BMD	Femoral length	AP femoral width	ML femoral width
Femoral BMD	798	0.07	0.008	0.05–0.10		0.551**	0.699**	0.120*	0.315**	0.294**
Vertebral BMD	797	0.06	0.006	0.04–0.08			0.708**	0.230**	0.319**	0.309**
Total BMD	799	0.05	0.004	0.04–0.06				0.223**	0.399**	0.372**
Femoral length	763	15.76	0.609	14.10–17.25					0.343**	0.253**
AP femoral width	790	1.39	0.097	1.16–1.68						0.547**
ML femoral width	790	1.88	0.150	1.45–2.32						

Note: Pearson partial correlations (controlling for parent of origin, sex, and body mass).
*$p < .05$, **$p < .0001$ following correction for multiple comparisons using the false-discovery-rate procedure (Curran-Everett, 2000).

many of the genetic determinants of AP also affect ML, but these are largely independent of factors affecting FL.

GRAIP-adjusted significant and suggestive loci for all skeletal architecture traits are presented in Table 2. Linkage analysis revealed one GRAIP-adjusted significant QTL on Chr. 3 for TBMD colocalizing with loci observed for FBMD and VBMD (Fig. 1*A*). This locus explained 3.0% of the total variance in TBMD. For VBMD, statistically significant loci were observed on chromosomes (Chrs.) 1, 3, and 5, collectively explaining 14.1% of the total phenotypic variation (Fig. 1*B*). The locus identified on Chr. 3 colocalized with that identified for FBMD. Significant additive effects were noted for the loci identified on Chrs. 1 and 5, with opposing allelic effects. In contrast, the contributions from additive and dominance effects were more equally balanced for the Chr. 3 QTL. For FBMD, two significant ($p \leq .05$, LOD ≥ 3.9) and one suggestive ($p \leq .1$, LOD ≥ 3.5) QTLs were observed (Fig. 1*C*). These QTLs collectively explained 5.6% of the total phenotypic variance, with additive and dominance effects varying by loci. No significant QTL $\times$ sex interactions were observed for TBMD, VBMD, or FBMD.

Regarding FL, significant loci were observed on Chrs. 1 and 5, collectively explaining 2.4% of the total phenotypic variation with relatively large average additive and dominance effects (Fig. 2*A*). Additionally, analyses of AP and ML femoral width resulted in eight significant and one suggestive QTLs on Chrs. 1, 2, 3, 4, 7, 8, 10, 13, and 15, with naive LOD scores ranging from 7.1 to 16.3 (Fig. 2*B*, *C*). Collectively, AP and ML width loci explained 22% and 9.8% of the total phenotypic variation. For AP width, allelic effects varied by locus, and additive and dominance effects generally were large and balanced. However, large average dominance effects, with little additively, were noted on Chrs. 13 and 15. While the significant dominance effect on Chr. 15 represented a decreasing effect in the heterozygote, a reversal was seen on Chr. 13, with an increasing effect in the heterozygote. For ML width, two (Chrs. 2 and 3) of the five loci were trait-specific QTLs, whereas signals observed on Chrs. 8, 10, and 13 were congruent with those observed for AP width. No significant QTL $\times$ sex interactions were observed for AP or ML femoral width.

The 1-LOD drop CIs for all QTLs ranged from 7 to 30 Mb. To identify putative candidate genes, we examined QTLs with narrow (<10 Mbp) CIs. Based on this analysis, we focused on the AP/ML QTL on Chr. 8 (Table 2) because it (1) was the most statistically significant (naive LOD = 16.3), (2) had the most narrow CI (101 to 107 Mb), and (3) was gene-sparse. Based on the NCBI37.1 genome build, this region harbored a total of 12 RefSeq protein-coding genes (*Cdh8*, *Cdh11*, *Cdh5*, *Bean1*, *Tk2*, *Cklf*, *Cmtm2a*, *Cmtm2b*, *Cmtm3*, *Cmtm4*, *Dync1li2*, and *Ccdc79*; Fig. 3*B*). The QTL peak was located just upstream of *Cdh11* at approximately 104 Mb (Fig. 3*B*).

Table 2. QTLs Detected and Respective Statistics for Skeletal Architecture Traits

Trait	Nearest marker	rs	MMU	Peak position (Mb)	Naive LOD	GRAIP LOD	CI (Mb)	% Variance	Additive ± SE	Dominance ± SE
Femoral BMD	JAX00098814	27504412	2	113	6.0	4.1*	107–115	2.2	−0.0018 ± 0.0004	−0.001 ± 0.001
	JAX00189293	50963474	3	125	6.4	4.2*	115–130	1.8	0.001 ± 0.001	0.001 ± 0.001
	JAX00133397	29583351	5	100	5.2	3.6	97–123	1.6	−0.0015 ± 0.0004	0.0003 ± 0.0006
Vertebral BMD	JAX00277411	48732938	1	179	7.5	4.2*	172–184	7.3	0.0022 ± 0.0003†	0.0003 ± 0.0004
	JAX00189293	50963474	3	126	7.8	4.0*	121–130	3.9	0.0014 ± 0.0003	0.0013 ± 0.0004
	JAX00581045	49523785	5	47	7.5	4.0*	43–52	2.9	−0.0014 ± 0.0003†	0.0004 ± 0.0004
Total BMD	JAX00189293	50963474	3	126	9.7	4.6*	122–130	3.0	0.0007 ± 0.0002	0.0008 ± 0.0003
Femoral length	JAX00002741	31930716	1	40	9.0	4.7*	35–63	0.3	−0.04 ± 0.03	−0.05 ± 0.04
	JAX00582506	48305016	5	53	9.9	4.7*	47–60	2.1	0.11 ± 0.03	0.09 ± 0.04
AP femoral width	JAX00005495	31575493	1	76	16.3	4.7*	72–80‡	0.6	−0.01 ± 0.01	0.01 ± 0.01
	JAX00567938	27582053	4	135	13.7	4.6*	124–139	3.5	0.02 ± 0.01	0.02 ± 0.01
	JAX00153077	31789816	7	76	10.0	4.4*	71–80	4.7	0.03 ± 0.01†	−0.01 ± 0.01
	JAX00165438	32321713	8	103	15.7	4.7*	101–107‡	7.1	−0.034 ± 0.004†	−0.0001 ± 0.0068
	JAX00021324	13480722	10	97	9.2	4.4*	87–103	1.4	−0.017 ± 0.005	0.003 ± 0.007
	JAX00041702	29736244	13	10	8.1	3.9*	−19	0.7	0.0002 ± 0.0049	0.02 ± 0.01
	JAX00395686	33859224	15	24	7.8	3.9*	−30	4.0	0.017 ± 0.004	−0.03 ± 0.01†
ML femoral width	JAX00100848	27189926	2	140	7.1	3.6	130–159	3.1	−0.03 ± 0.01†	0.02 ± 0.01
	JAX00107680	30641053	3	56	8.0	4.4*	46–68	1.2	0.02 ± 0.01	−0.003 ± 0.011
	JAX00165438	32321713	8	103	12.1	4.7*	100–107‡	4.0	−0.04 ± 0.01†	0.02 ± 0.01
	JAX00021324	13480722	10	97	9.2	4.7*	90–107	1.4	−0.02 ± 0.01	−0.01 ± 0.01
	JAX00041702	29736244	13	10	11.6	4.7*	−14‡	0.1	−0.01 ± 0.01	0.01 ± 0.01

Note: LOD scores exceeding the 95% ($p = .05$, LOD ≥ 3.9) permutation threshold are denoted by asterisk; other QTLs exceeded the 90% ($p = .1$, LOD ≥ 3.5) threshold. Confidence intervals (CIs) for QTL positions were obtained using a 1-LOD drop in megabases. Marker positions are based on Mouse Build 36 of the Mouse Diversity Genotyping Array. CIs are relative to the GRAIP-permuted LOD score with the exception of those denoted by ‡, which are relative to the naive LOD score. Percent variance is the percentage of phenotypic variance accounted for by the QTL effect. For additive and dominance effects, positive values indicate increasing effect of the HR allele or increasing effect of the heterozygote, respectively. †Indicates that additive and dominance effects were statistically significant at $p < .05$.

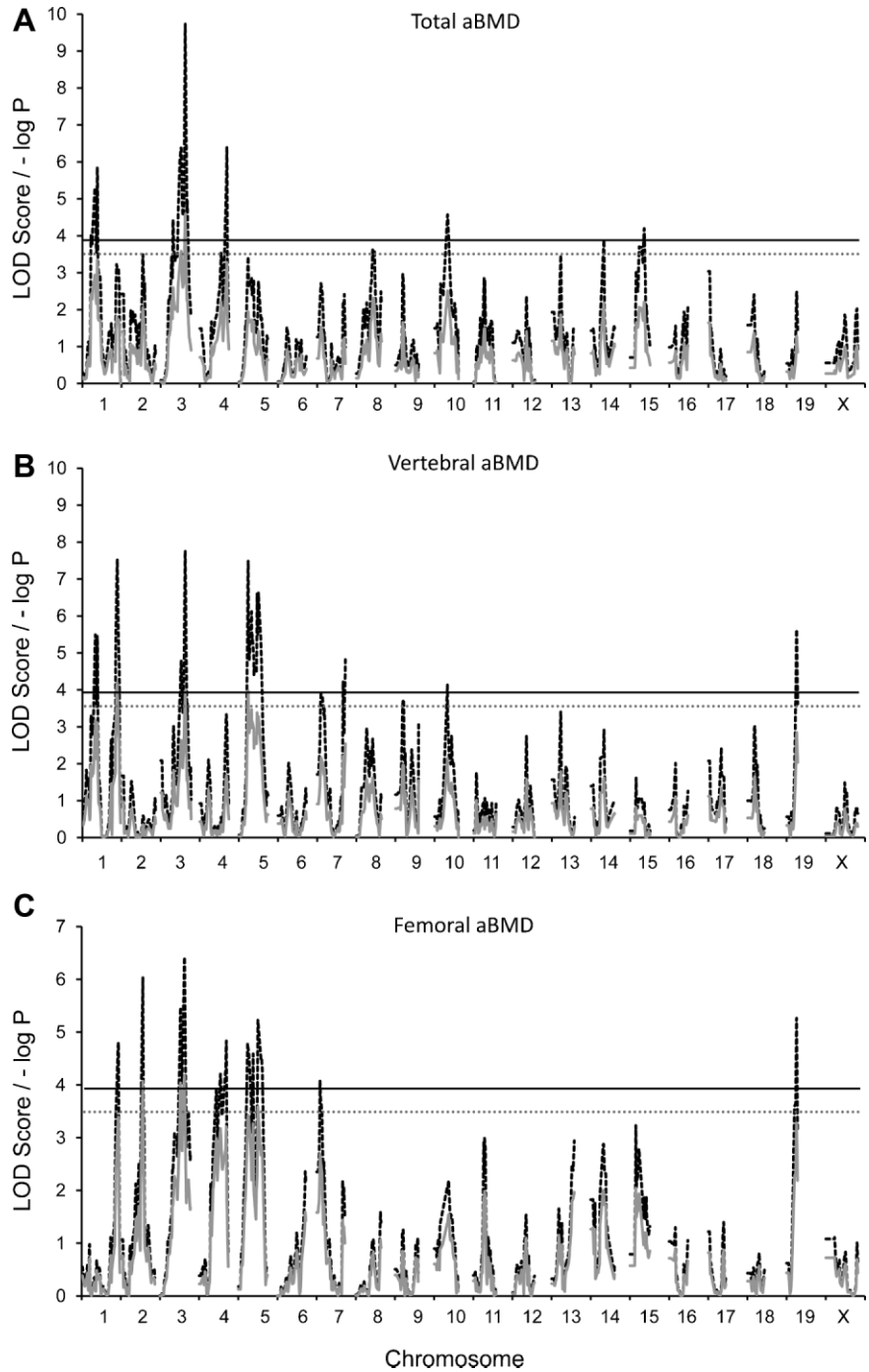

Fig. 1. G_4 QTL maps of (*A*) total aBMD, (*B*) vertebral aBMD, and (*C*) femoral aBMD. Red traces are the simple mapping output, and black traces are GRAIP permutation output. For the GRAIP output, a minimum possible *p* value with 50,000 permutations is .00002 (1/50,000), so the maximum $-\log p = 4.7$. The black and gray lines represent the permuted 95% (LOD $\geq$ 3.9, $p \leq .05$) and 90% (LOD $\geq$ 3.5, $p \leq 0.1$) LOD thresholds, respectively.

Next, we characterized the pattern of haplotype diversity in the founders for this region to prioritize candidate genes. Approximately half the region (49.5%) is IBD among B6 and all 12 HR founders. Given that these regions are IBD, they are not likely to harbor QTLs; therefore, our analysis confined the QTLs to three regions that account for the other half of the original candidate region (Fig. 3*C*). Of the 12 candidate genes, the coding regions of 7 (*Cdh8*, *Cdh5*, *Bean1*, *Tk2*, *Cklf*, *Cmtm2a*, and *Cmtm2b*) were located within IBD regions and can be excluded, whereas 5 (*Cdh11*, *Cmtm3*, *Cmtm4*, *Dync1li2*, and *Ccdc79*) were located in segregating regions and therefore are now of a higher priority (Fig. 3*C*).

It is likely that the gene responsible for the effects on femoral width on Chr. 8 is expressed in osteoblasts and/or osteoclasts, the cells responsible for the bone modeling and remodeling that determines femoral morphology in adult mice.[33] Therefore, we surveyed publically available microarray expression data on primary osteoblasts (at 5, 14, and 21 days of differentiation) and osteoclasts (http://biogps.gnf.org[29,34]) to determine which, if any, of the 12 candidates were expressed in these cells. Of the 12,

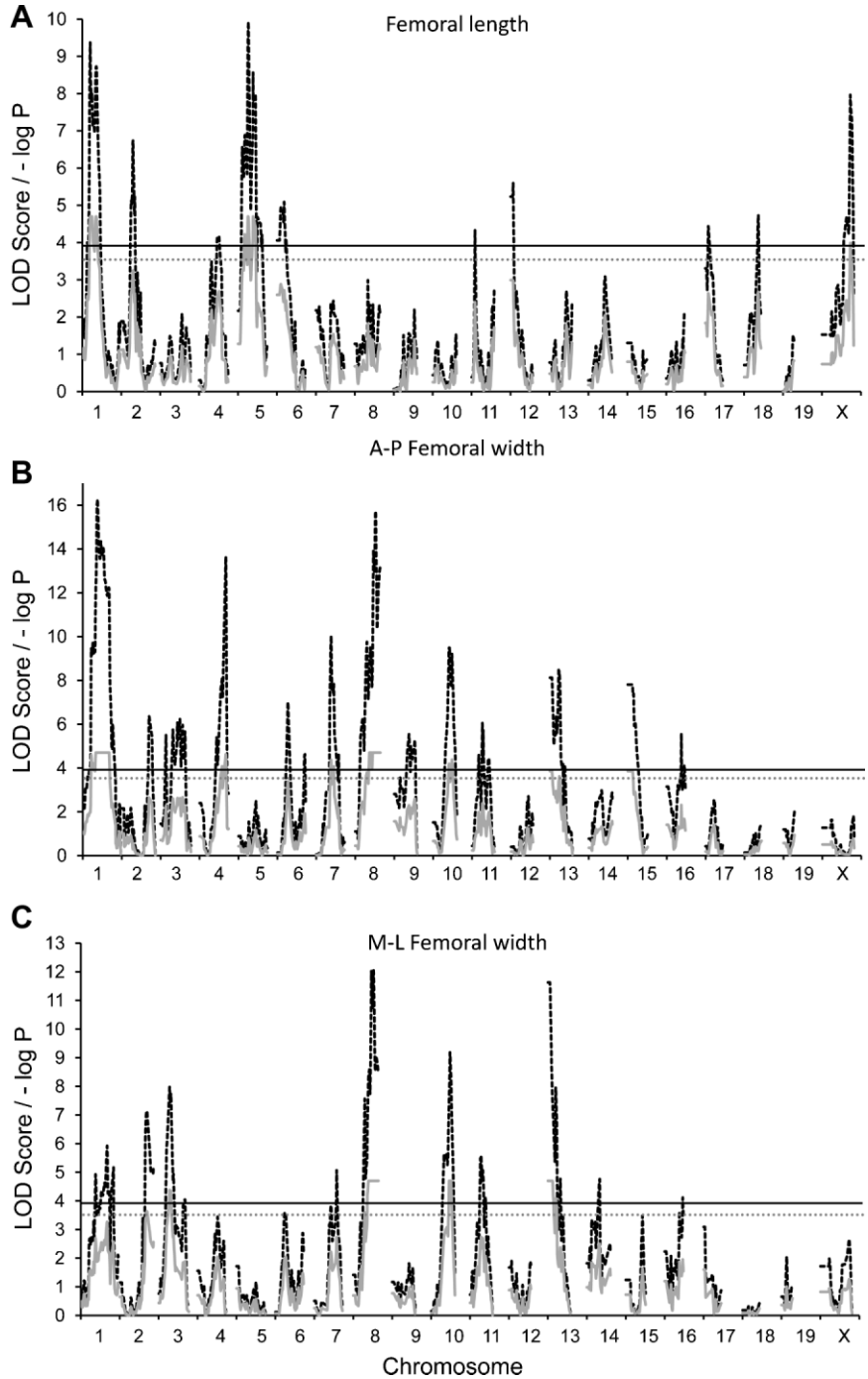

Fig. 2. G_4 QTL maps of (*A*) femoral length, (*B*) anteroposterior femoral width, and (*C*) mediolateral femoral width. Red traces are the simple mapping output, and black traces are GRAIP permutation output. For the GRAIP output, a minimum possible *p* value with 50,000 permutations is .00002 (1/50,000), so the maximum –log $p = 4.7$. The black and gray lines represent the permuted 95% (LOD ≥ 3.9, $p \leq 05$) and 90% (LOD ≥ 3.5, $p \leq 0.1$) LOD thresholds, respectively.

microarray data were available for all except *Cmtm4*. As shown in Fig. 4, five (*Cdh11*, *Tk2*, *Cklf*, *Cmtm3*, and *Dync1li2*) were expressed in osteoblasts and/or osteoclasts. *Cdh11* demonstrated the highest expression in any of the two cell types, and its expression was increased significantly ($p < .05$) as a function of osteoblast differentiation (expression on days 14 and 21 was increased relative to day 5). The expression of the other four did not differ statistically ($p > .05$) across the osteoblast differentiation time course. Together, the IBD data and gene expression profiles of the genes in the QTL CI are consistent with variation within *Cdh11* being the basis of the Chr. 8 AP and ML QTL.

Discussion

Traits that contribute to bone strength are under strong genetic regulation.[4] Therefore, identification of novel genes that regulate these phenotypes promises to highlight the key

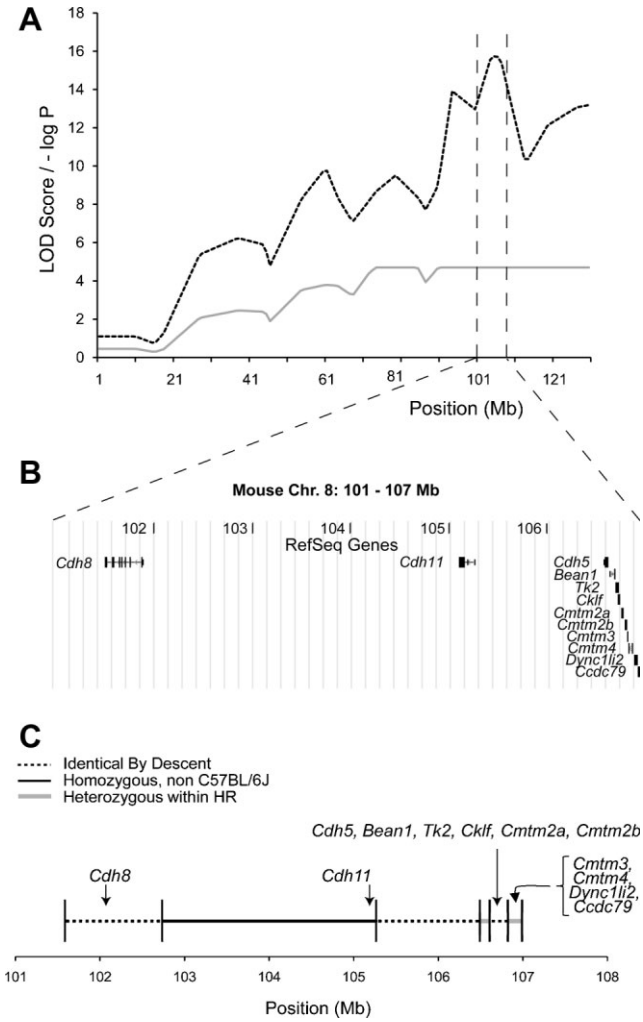

Fig. 3. Haplotype diversity analysis narrows QTLs to three non-IBD regions. The panels present (*A*) the naive and GRAIP-adjusted AP LOD score profiles across Chr. 8, (*B*) the RefSeq gene content within, and (*C*) the IBD assignments across the 6-Mb 1-LOD QTL CI.

biologic processes that contribute to bone fragility. In this study, we used a novel mouse AIL to identify 16 QTLs affecting aBMD and femoral geometry phenotypes. One of the key observations from this study was that an AP/ML femoral width QTL on Chr. 8 was most likely the result of variation in *Cdh11*.

One of the limitations of genetic analysis in the mouse is that the most commonly used experimental crosses (eg, an F_2 cross) suffer from a lack of resolution.[9] Recently, a number of groups have begun to explore the use of higher-resolution approaches that identify QTLs with more narrow CIs using populations such as advanced intercross lines (AILs).[10–12] AILs are created by randomly mating mice derived from two parental strains for multiple generations.[13] The accumulation of recombination events during each round of meiosis results in mice whose genomes are fined-grained mosaics of the two founder strains. These extra recombinations increase the precision of QTL localization, resulting in the confinement of QTLs to smaller genomic intervals, which aids in elucidation of the underlying genes.[13]

As discussed earlier, the G_4 AIL has the significant advantage of improved mapping resolution over more traditional approaches. Owing to the accumulation of additional recombination events, the genetic map in the G_4 was expanded by approximately a factor of 3 relative to an equivalent F_2.[10] To put this into context, we calculated the size of the 95% CIs for the 150 BMD QTLs indentified in F_2 crosses recently reported by Ackert-Bicknell and colleagues.[35] The average F_2 CI was 49.8 ± 2.3 Mb compared with 12.4 ± 6.5 Mb for the aBMD QTL identified in our G_4 AIL. Although this comparison is not entirely appropriate owing to differences in statistical power and the way the CIs were calculated, it still demonstrates the improvement in resolution. To our knowledge, only one other group has used an AIL to study the genetics of bone traits. Recently, Norgard and colleagues used an F_2–F_3 population ($n = \sim 2000$) derived from the LG/J and SM/J inbred strains of mice to identify QTLs affecting the lengths of the humerus, ulna, femur, and tibia.[7] The authors identified 70 QTLs affecting bone-length traits. None of the femoral length QTLs identified by Norgard and colleagues overlapped with FL loci identified in this study. It is, however, not uncommon for

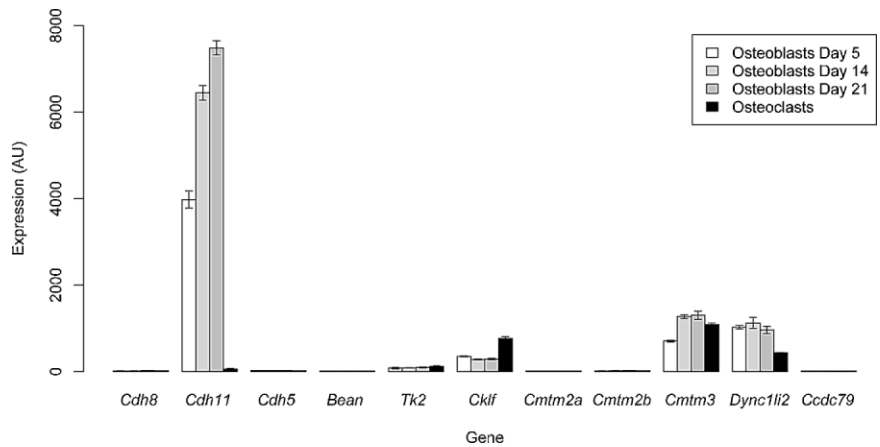

Fig. 4. Gene expression analysis for QTL genes in primary calvarial osteoblasts at 5, 14, and 21 days of differentiation and osteoclasts. The mean ± SEM of two microarray replicates per sample are plotted. Of the five genes that show detectable expression (*Cdh11*, *Tk2*, *Cklf*, *Cmtm3*, and *Dync1li2*) in osteoblasts, *Cdh11* is the only gene that is statistically different ($p < .05$) across the time course.

distinct sets of QTLs to be identified in different mouse crosses, and this is likely due to the segregation of unique genetic variation in each cross, different ages at measurement, different environmental conditions, and/or differences in statistical power in the two studies. In a subsequent study, the bone-length QTLs identified by Norgard and colleagues were fine-mapped using F_9–F_{10} AIL mice from the same population.[36] The use of F_9–F_{10} mice resulted in a significant increase in mapping resolution. Their average 95% CI was approximately 1.7 F_2 cM or approximately 3.4 Mb and encompassed, on average, 35 genes compared with 275 per CI in the F_2–F_3 population.[36] This later study demonstrates the significant improvement in mapping resolution that can be obtained using later-generation AIL mice.

Differences in the genetic regulation of aBMD at various skeletal sites have been observed in previous mouse mapping studies.[37–40] We observed similar results for TBMD, VBMD, and FBMD in this study. Only the locus on Chr. 3 regulated all three traits. In some cases, this may be due to differences in effect sizes across traits. For example, on the distal end of Chr. 1, the LOD score for FBMD is just below the significance threshold in the location of a significant VBMD QTL (Fig. 1). We did, however, observe examples of site-specific QTLs, such as the Chr. 2 FBMD QTL. The naive LOD score for FBMD on Chr. 2 at 113 Mb was 6.0, whereas the LOD score in the same location was less than 1.0 for VBMD (Fig. 1). These results confirm that aBMD at different skeletal sites is under both common and unique genetic regulation.

A number of QTL mapping studies for aBMD have been performed in the mouse, resulting in the identification of hundreds of loci.[5,6] Based on data from a recent review[6] and meta-analysis,[5] we determined that all five peak aBMD QTL markers identified herein overlapped with the 95% CI for a previously identified BMD QTL. In particular, the Chr. 1 VBMD QTL overlapped with QTLs identified in at least seven different studies.[6] This region appears to be a hotspot for BMD QTLs, and congenic strain analyses have demonstrated that the distal region of Chr.1 harbors multiple linked BMD loci.[41,42] One such locus is the bone mineral density 1 (*Bmd1*) QTL discovered by Beamer and colleagues in an F_2 cross between the CAST/EiJ and B6 inbred strains. Recently, the *duffy antigen receptor for chemokines* (*Darc*) gene was identified to be at least partially responsible for the effects of *Bmd1*.[43] In addition, the same group has used congenic strains to fine map a second separate QTL, just distal of *Darc*, down to a 0.152-Mb region containing two candidates, *absent in melanoma 2* (*Aim2*) and *AC084073.22*.[41]

Although fewer studies have investigated the genetic basis of femur geometry, we did identify overlap between loci identified in this study and previously detected QTLs affecting the same or similar traits. To identify previously known QTLs, we searched the Mouse Genome Informatics (MGI; www.informatics.jax.org) QTL database. This search did not identify any overlap with previously identified QTLs for FL. However, of the nine unique femur width QTLs, the peak markers for six were found to lie within the CIs of previously identified QTLs affecting femur geometry and/or femoral biomechanical traits. Of the six, overlaps with the QTLs on Chrs. 4 and 8 were of particular interest. In a number of studies, the distal end of Chr. 4 has been found to harbor large-effect QTLs influencing many bone-strength phenotypes.[37,42,44–48] Most QTLs in this region have peaks between 130 and 140 Mb. In our study, we identified a significant AP QTL at 135 Mb (Table 2). In addition, QTLs with significant naive LOD scores that failed to reach significant after the GRAIP adjustment were identified for FBMD and TBMD at 139 Mb (data not shown). Although this region has been identified as a bone QTL hotspot, the underlying gene(s) have not been identified. Mapping efforts are complicated in this region by an extremely high gene density. The 10-Mb interval from 130 to 140 Mb on Chr. 4 contains 213 RefSeq genes, a density (21.3 genes/Mb) that is roughly three times the genome average (~7 genes/Mb). Given that the G_4 segregates for variation affecting femoral bone traits in this region, the analysis of mice from the G_{10} or later may provide the added resolution needed to identify the responsible gene(s). This is especially important given that the syntenic human region has been implicated in the regulation of BMD in recent GWA studies.[8,49]

Although previously identified QTLs specifically for AP and ML have not been observed for the Chr. 8 AP/ML locus, this region of Chr. 8 appears to be a hotspot for similar bone structure and strength trait QTLs. Among the overlaps, Klein and colleagues identified the *femoral cross-sectional area 2* (*Fcsa2*) QTL at 89 Mb affecting femoral cross-sectional area (FCSA) in an F_2 cross between B6 and DBA/2J mice.[50] In that study, as well as in this study, the B6 allele increased trait means. A second FCSA locus was identified at 90 Mb by Volkman and colleagues in the progeny of a cross between (BALB/cJ × C57BL/6J) F_1 females and (C3H/HeJ × DBA/2J) F_1 males.[51] Additionally, Koller and colleagues identified the *femoral bone trait QTL 3* (*Fbtq3*) located at 119 Mb in a cross between B6 and C3H/HeJ mice.[46] This locus affected femoral polar moment of interia (I_p), stiffness (S), and load to failure (F_u). B6 alleles were associated with larger I_p, S, and F_u values. This region also has been found to harbor QTLs affecting changes in tibial BMD, periosteal circumference, and cortical thickness and the transcript levels of the bone marker genes *bone sialoprotein* (*Bsp*) and *alkaline phosphatase* (*Akp2*) in response to mechanical loading.[52,53] These data suggest that this region of Chr. 8 contains variants that affect many aspects of bone density, structure, strength, and mechanical responsiveness. As will be discussed below, our genetic data suggest that *Cdh11* is at least partially responsible for these effects.

To identify candidate genes, we performed a detailed investigation of the genes within the Chr. 8 AP/ML QTL CI. This locus was chosen because it was the most statistically significant and had the smallest CI. It also turned out that this region was gene-sparse, increasing our odds of being able to prioritize among candidates. A total of 12 genes were located in the CI, and at approximately 2 genes/Mb, it had a lower gene density than the genome average (~7 genes/Mb). Three lines of evidence suggest that of the 12 genes, *Cdh11* is likely the causal gene for the bone QTLs discovered in these (and possibly other) studies: (1) It was located within a non-B6 haplotype in the HR founders, (2) it was highly expressed in primary osteoblasts and was the only gene whose expression differed as a function of osteoblast differentiation, and (3) it was the only gene in the region previously implicated in bone development. It is important to note that *Cdh11* also has been suggested as a candidate for

the mouse tibial mechanical responsiveness QTLs described earlier[52,53] and for a QTL affecting alterations in the contour of the navicular bones in horses.[54]

Cdh11 encodes cadherin 11 (also known as *osteoblast cadherin*) and is thought to play an important role in mediating cell-cell adhesion in the skeleton.[55] Cadherin 11 and *N*-cadherin (encoded by *Cdh2*) are the major cadherin family members expressed in bone-forming osteoblasts.[56,57] A role for *Cdh11* in osteoblast function was demonstrated recently by the observation that osteoblast differentiation was defective in primary calvarial osteoblasts isolated from *Cdh11*-deficient (*Cdh11*$^{-/-}$) mice.[58,59] However, in adult *Cdh11*$^{-/-}$ mice, the only observed skeletal defect was modest osteopenia.[58,59] It has been hypothesized that the lack of a more severe in vivo skeletal phenotype may be due to functional compensation by *N*-cadherin in osteoblasts.[59] In support of this hypothesis, double *Cdh2/Cdh11* knockout mice have significantly reduced BMD and femoral cross-sectional area, and the latter is a phenotype that would be captured by the AP and/or ML measurements obtained in this study.[59] The double-knockout data indicate that in the "correct" genetic background perturbation of *Cdh11* alters femoral width. Therefore, it is possible that the genetic background in the G_4 (owing to mutations in *Cdh2* or other unknown "enabling" loci) provides an environment in which functional variation within *Cdh11* leads to alterations in femur width. Although these data strongly suggest that *Cdh11* is the causal gene, other possibilities do exist. For instance, one of the four other genes in the non-IBD regions could be causal, or regulatory variation in the non-IBD regions may be altering the expression of other genes in the region. It is also possible that multiple causal linked genes exist. Additional work is needed to confirm our hypothesis that *Cdh11* is the responsible gene.

In conclusion, we have used a G_4 AIL to identify regions of the mouse genome that regulate aBMD and femur morphology. The use of an AIL resulted in significantly reduced CIs compared with an F_2 cross. In addition, by combining QTL mapping data, microarray data, and an IBD analysis, *Cdh11* was identified as a likely regulator of femoral morphology. These results lay the groundwork for the ultimate discovery of causal genes, and their identification promises to increase our understanding of genes and pathways that regulate bone strength.

Disclosures

All the authors state that they have no conflicts of interest.

Acknowledgments

We thank Z Yun for assistance with animal care and data collection and KM Middleton for insightful comments on the manuscript. This work was supported by NIH Grant DK076050 to DP. SAK was supported through an NIMH-funded (5T32MH075854-04) Interdisciplinary Obesity Training (IDOT) program. Phenotypes were collected in part using the Animal Metabolism Phenotyping core facility within UNC's Clinical Nutrition Research Center (funded by NIDDK Grant DK056350). CRF and SAK contributed equally to this work.

Authors' roles: CRF, SAK, TA, and DP conceived and designed the study. SAK, EB, DY, KH, DLN, and RJB performed the experiments. CRF, SAK, FPDV, RJB, and DP analyzed the data. CRF, SAK, TG, and DP drafted the manuscript. CRF and DP provided oversight of the project. All authors read and approved the final manuscript.

References

1. Gilsanz V, Loro ML, Roe TF, Sayre J, Gilsanz R, Schulz EE. Vertebral size in elderly women with osteoporosis: mechanical implications and relationship to fractures. J Clin Invest. 1995;95:2332–2337.
2. Ng AH, Wang SX, Turner CH, Beamer WG, Grynpas MD. Bone quality and bone strength in BXH recombinant inbred mice. Calcif Tissue Int. 2007;81:215–223.
3. Johnell O, Kanis JA, Oden A, et al. Predictive value of BMD for hip and other fractures. J Bone Miner Res. 2005;20:1185–1194.
4. Peacock M, Turner CH, Econs MJ, Foroud T. Genetics of osteoporosis. Endocr Rev. 2002;23:303–326.
5. Ackert-Bicknell CL, Karasik D, Li Q, et al. Mouse BMD quantitative trait loci show improved concordance with human genome wide association loci when recalculated on a new, common mouse genetic map. J Bone Miner Res. 2010;25:1808–1820.
6. Xiong Q, Jiao Y, Hasty KA, et al. Quantitative trait loci, genes, and polymorphisms that regulate bone mineral density in mouse. Genomics. 2009;93:401–414.
7. Norgard EA, Roseman CC, Fawcett GL, et al. Identification of quantitative trait loci affecting murine long bone length in a two-generation intercross of LG/J and SM/J Mice. J Bone Miner Res. 2008;23:887–895.
8. Rivadeneira F, Styrkarsdottir U, Estrada K, et al. Twenty bone-mineral-density loci identified by large-scale meta-analysis of genome-wide association studies. Nat Genet. 2009;41:1199–1206.
9. Flint J, Valdar W, Shifman S, Mott R. Strategies for mapping and cloning quantitative trait genes in rodents. Nat Rev Genet. 2005;6:271–286.
10. Kelly SA, Nehrenberg DL, Peirce JL, et al. Genetic architecture of voluntary exercise in an advanced intercross line of mice. Physiol Genomics. 2010;42:190–200.
11. Fawcett GL, Jarvis JP, Roseman CC, Wang B, Wolf JB, Cheverud JM. Fine-mapping of obesity-related quantitative trait loci in an F9/10 advanced intercross line. Obesity (Silver Spring). 2010;18:1383–1392.
12. Yu X, Bauer K, Wernhoff P, Ibrahim SM. Using an advanced intercross line to identify quantitative trait loci controlling immune response during collagen-induced arthritis. Genes Immun. 2007;8:296–301.
13. Darvasi A, Soller M. Advanced intercross lines, an experimental population for fine genetic mapping. Genetics. 1995;141:1199–1207.
14. Kelly SA, Nehrenberg DL, Hua K, Gordon RR, Garland T Jr, Pomp D. Parent-of-origin effects on voluntary exercise levels and body composition in mice. Physiol Genomics. 2010;40:111–120.
15. Swallow JG, Carter PA, Garland T Jr. Artificial selection for increased wheel-running behavior in house mice. Behav Genet. 1998;28:227–237.
16. Kelly SA, Czech PP, Wight JT, Blank KM, Garland T Jr. Experimental evolution and phenotypic plasticity of hindlimb bones in high-activity house mice. J Morphol. 2006;267:360–374.
17. Middleton KM, Shubin CE, Moore DC, Carter PA, Garland T Jr, Swartz SM. The relative importance of genetics and phenotypic plasticity in dictating bone morphology and mechanics in aged mice: evidence from an artificial selection experiment. Zoology (Jena). 2008;111:135–147.
18. Middleton KM, Goldstein BD, Guduru PR, et al. Variation in within-bone stiffness measured by nanoindentation in mice bred

for high levels of voluntary wheel running. J Anat. 2010;216:121–131.

19. Wallace IJ, Middleton KM, Lublinsky S, et al. Functional significance of genetic variation underlying limb bone diaphyseal structure. Am J Phys Anthropol. 2010;143:21–30.
20. Lopez Franco GE, O'Neil TK, Litscher SJ, Urban-Piette M, Blank RD. Accuracy and precision of PIXImus densitometry for ex vivo mouse long bones: comparison of technique and software version. J Clin Densitom. 2004;7:326–333.
21. Curran-Everett D. Multiple comparisons: philosophies and illustrations. Am J Physiol Regul Integr Comp Physiol. 2000;279:R1–8.
22. Peirce JL, Broman KW, Lu L, et al. Genome Reshuffling for Advanced Intercross Permutation (GRAIP): simulation and permutation for advanced intercross population analysis. PLoS One. 2008;3:e1977.
23. Valdar W, Holmes CC, Mott R, Flint J. Mapping in structured populations by resample model averaging. Genetics. 2009;182:1263–77.
24. Benson AK, Kelly SA, Legge R, et al. Individuality in gut microbiota composition is a complex polygenic trait shaped by multiple environmental and host genetic factors. Proc Natl Acad Sci U S A. 2010;107:18933–18938.
25. Broman KW, Wu H, Sen S, Churchill GA. R/qtl: QTL mapping in experimental crosses. Bioinformatics. 2003;19:889–890.
26. Team RDC. *R: A Language and Environment for Statistical Computing*. Vienna, Austria: R Foundation for Statistical Computing, 2008.
27. Sen S, Churchill GA. A statistical framework for quantitative trait mapping. Genetics. 2001;159:371–87.
28. Peirce JL, Broman KW, Lu L, Williams RW. A simple method for combining genetic mapping data from multiple crosses and experimental designs. PLoS One. 2007;2:e1036.
29. Lattin JE, Schroder K, Su AI, et al. Expression analysis of G Protein-Coupled Receptors in mouse macrophages. Immunome Res. 2008;4:5.
30. Gautier L, Cope L, Bolstad BM, Irizarry RA. affy--analysis of Affymetrix GeneChip data at the probe level. Bioinformatics. 2004;20:307–15.
31. Irizarry RA, Hobbs B, Collin F, et al. Exploration, normalization, and summaries of high density oligonucleotide array probe level data. Biostatistics. 2003;4:249–264.
32. Yang H, Ding Y, Hutchins LN, et al. A customized and versatile high-density genotyping array for the mouse. Nat Methods. 2009;6:663–666.
33. Seeman E, Delmas PD. Bone quality--the material and structural basis of bone strength and fragility. N Engl J Med. 2006;354:2250–2261.
34. Wu C, Orozco C, Boyer J, et al. BioGPS: an extensible and customizable portal for querying and organizing gene annotation resources. Genome Biol. 2009;10:R130.
35. Ackert-Bicknell CL, Karasik D, Li Q, et al. Mouse BMD quantitative trait loci show improved concordance with human genome-wide association loci when recalculated on a new, common mouse genetic map. J Bone Miner Res. 2010;25:1808–20.
36. Norgard EA, Jarvis JP, Roseman CC, et al. Replication of long-bone length QTL in the F9-F10 LG,SM advanced intercross. Mamm Genome. 2009;20:224–235.
37. Beamer WG, Shultz KL, Donahue LR, et al. Quantitative trait loci for femoral and lumbar vertebral bone mineral density in C57BL/6J and C3H/HeJ inbred strains of mice. J Bone Miner Res. 2001;16:1195–1206.
38. Ishimori N, Li R, Walsh KA, et al. Quantitative trait loci that determine BMD in C57BL/6J and 129S1/SvImJ inbred mice. J Bone Miner Res. 2006;21:105–112.
39. Ishimori N, Stylianou IM, Korstanje R, et al. Quantitative trait loci for BMD in an SM/J by NZB/BlNJ intercross population and identification of Trps1 as a probable candidate gene. J Bone Miner Res. 2008;23:1529–1537.
40. Masinde GL, Li X, Gu W, Wergedal J, Mohan S, Baylink DJ. Quantitative trait loci for bone density in mice: the genes determining total skeletal density and femur density show little overlap in F2 mice. Calcif Tissue Int. 2002;71:421–428.
41. Beamer WG, Shultz KL, Coombs HF 3rd, et al. BMD regulation on mouse distal chromosome 1, candidate genes, and response to ovariectomy or dietary fat. J Bone Miner Res. 2011;26:88–99.
42. Shultz KL, Donahue LR, Bouxsein ML, Baylink DJ, Rosen CJ, Beamer WG. Congenic strains of mice for verification and genetic decomposition of quantitative trait loci for femoral bone mineral density. J Bone Miner Res. 2003;18:175–185.
43. Edderkaoui B, Baylink DJ, Beamer WG, et al. Identification of mouse Duffy antigen receptor for chemokines (Darc) as a BMD QTL gene. Genome Res. 2007;17:577–585.
44. Jiao F, Chiu H, Jiao Y, et al. Quantitative trait loci for tibial bone strength in C57BL/6J and C3H/HeJ inbred strains of mice. J Genet. 2010;89:21–27.
45. Saless N, Lopez Franco GE, Litscher S, et al. Linkage mapping of femoral material properties in a reciprocal intercross of HcB-8 and HcB-23 recombinant mouse strains. Bone. 2010;46:1251–1259.
46. Koller DL, Schriefer J, Sun Q, et al. Genetic effects for femoral biomechanics, structure, and density in C57BL/6J and C3H/HeJ inbred mouse strains. J Bone Miner Res. 2003;18:1758–1765.
47. Bouxsein ML, Uchiyama T, Rosen CJ, et al. Mapping quantitative trait loci for vertebral trabecular bone volume fraction and microarchitecture in mice. J Bone Miner Res. 2004;19:587–599.
48. Farber CR, van Nas A, Ghazalpour A, et al. An integrative genetics approach to identify candidate genes regulating BMD: combining linkage, gene expression, and association. J Bone Miner Res. 2009;24:105–116.
49. Styrkarsdottir U, Halldorsson BV, Gretarsdottir S, et al. Multiple genetic loci for bone mineral density and fractures. N Engl J Med. 2008;358:2355–2365.
50. Klein RF, Turner RJ, Skinner LD, et al. Mapping quantitative trait loci that influence femoral cross-sectional area in mice. J Bone Miner Res. 2002;17:1752–1760.
51. Volkman SK, Galecki AT, Burke DT, Miller RA, Goldstein SA. Quantitative trait loci that modulate femoral mechanical properties in a genetically heterogeneous mouse population. J Bone Miner Res. 2004;19:1497–1505.
52. Kesavan C, Baylink DJ, Kapoor S, Mohan S. Novel loci regulating bone anabolic response to loading: expression QTL analysis in C57BL/6JXC3H/HeJ mice cross. Bone. 2007;41:223–230.
53. Kesavan C, Mohan S, Srivastava AK, et al. Identification of genetic loci that regulate bone adaptive response to mechanical loading in C57BL/6J and C3H/HeJ mice intercross. Bone. 2006;39:634–643.
54. Diesterbeck US, Hertsch B, Distl O. Genome-wide search for microsatellite markers associated with radiologic alterations in the navicular bone of Hanoverian warmblood horses. Mamm Genome. 2007;18:373–381.
55. Mbalaviele G, Shin CS, Civitelli R. Cell-cell adhesion and signaling through cadherins: connecting bone cells in their microenvironment. J Bone Miner Res. 2006;21:1821–1827.
56. Cheng SL, Lecanda F, Davidson MK, et al. Human osteoblasts express a repertoire of cadherins, which are critical for BMP-2-induced osteogenic differentiation. J Bone Miner Res. 1998;13:633–644.
57. Okazaki M, Takeshita S, Kawai S, et al. Molecular cloning and characterization of OB-cadherin, a new member of cadherin family expressed in osteoblasts. J Biol Chem. 1994;269:12092–12098.
58. Kawaguchi J, Azuma Y, Hoshi K, et al. Targeted disruption of cadherin-11 leads to a reduction in bone density in calvaria and long bone metaphyses. J Bone Miner Res. 2001;16:1265–1271.
59. Di Benedetto A, Watkins M, Grimston S, et al. N-cadherin and cadherin 11 modulate postnatal bone growth and osteoblast differentiation by distinct mechanisms. J Cell Sci. 2010;123:2640–2648.